PAPER

Phase separation in $Ca_{1-x}La_xFe_2As_2$ superconductors: a ^{57}Fe Mössbauer study

To cite this article: Xiaoxing Liu *et al* 2016 *J. Phys.: Condens. Matter* **28** 125701

IOP Publishing Journal of Physics: Condensed Matter
J. Phys.: Condens. Matter **28** (2016) 125701 (7pp) doi:10.1088/0953-8984/28/12/125701

Phase separation in $Ca_{1-x}La_xFe_2As_2$ superconductors: a ^{57}Fe Mössbauer study

Xiaoxing Liu, Yang Li, Jianmei Wan, Zhiwei Li and Hua Pang

Institute of Applied Magnetics, Key Laboratory for Magnetism and Magnetic Materials of the Ministry of Education, Lanzhou University, Lanzhou 730000, People's Republic of China

E-mail: hpang@lzu.edu.cn

Received 24 November 2015, revised 20 January 2016
Accepted for publication 21 January 2016
Published 24 February 2016

Abstract

We report a detailed ^{57}Fe Mössbauer study of lanthanum doped $CaFe_2As_2$ superconductors. The quadrupole splitting distribution (QSD) method was adopted to analyze the Mössbauer spectra of $Ca_{1-x}La_xFe_2As_2$ ($x = 0.2, 0.3$) single crystals. For both compounds we observed two QSD contributions centered at 0.31 mm s^{-1} and -0.32 mm s^{-1} at room temperature. The first principles calculations of the electronic structures and the electric field gradient (EFG) of $Ca_{1-y}La_yFe_2As_2$ model systems reveal that the EFG changes from positive to negative with increasing dopant concentration, indicating that the La atoms distribute heterogeneously in the compounds. The two QSD components behave differently with decreasing temperature. The minority La-rich phase undergoes superconducting transition, while short range spin fluctuations and/or spin-phonon coupling appear in the majority La-poor phase. Our experiments provide new evidence of the phase separation picture at low temperatures in $Ca_{1-x}La_xFe_2As_2$ superconductors.

Keywords: iron-based superconductors, $Ca_{1-x}La_xFe_2As_2$, ^{57}Fe Mössbauer study

(Some figures may appear in colour only in the online journal)

Introduction

The discovery of iron-based superconductors rekindles research interest on the magnetic order, spin excitations, and their relationship with superconductivity, which has long been a focus in the search for the mechanism of high temperature superconductivity. In iron pnictides and iron chalcogenides, superconductivity usually occurs adjacent to an antiferromagnetic (AF) phase and overlapping region of the two orders on the doping phase diagram has been reported for these materials [1–5]. Though experimental observations and theoretical calculations have pointed out the importance of spin fluctuations, resulting from Fermi surface nesting between hole and electron pockets, for the formation of superconducting pairs in iron pnictides [6–8], high temperature superconducting phase far separated from the AF phase has also been observed in $LaFeAsO_{1-x}H_x$ [9] and $(Tl,Rb,K)_{1-x}Fe_{2-y}Se_2$ [10].This separation also happens in the extensively studied 122 family of iron pnictides [11].

Very recently, several research groups report superconducting phase with Tc around 40 ~ 49 K in rare earth-doped $CaFe_2As_2$ (Re = La, Ce, Nd, and Pr) and in La and P co-doped $CaFe_2As_2$ [11–14]. These observations suggest the flexibility in realizing superconductivity for 122 family pnictides. The common ground of these compounds is that the high temperature superconductivity occurs in sufficiently doped samples. Besides, the comparatively very small superconducting volume is also a distinguishing feature. Though bulk superconductivity can be realized by substituting alkaline earths by alkali metals (hole doping), Fe element by transition metal such as Co and Ni(electron doping), and P for As (isovalent doping) in 122 compounds, full volume fraction screening has never been observed in Re-doped $CaFe_2As_2$ compounds. Up to now, the nature of the superconducting state in these compounds is a controversial issue [15, 16]. To the best of our knowledge, it is still unclear whether slow magnetic fluctuations or disordered magnetism exist in these superconductors. In this respect, a microscopic investigation of the Re-doped

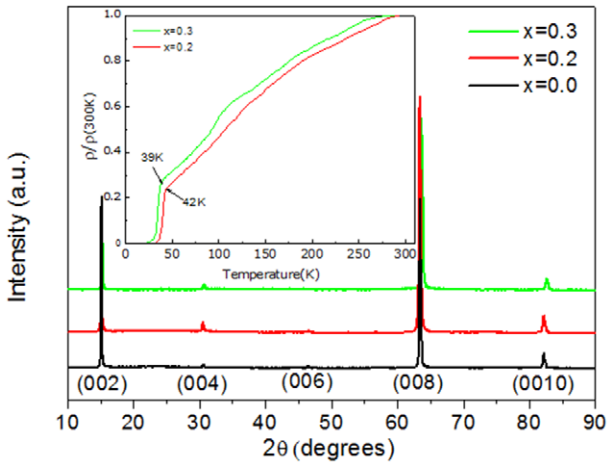

Figure 1. X-ray diffraction patterns of the single crystals $Ca_{1-x}La_xFe_2As_2$ ($x = 0.0$, 0.2, 0.3). The inset shows the normalized electrical resistivity as a function of temperature of the $Ca_{1-x}La_xFe_2As_2$($x = 0.2$, 0.3) crystals.

$Ca_{1-x}Re_xFe_2As_2$ by Mössbauer spectroscopy, which has been proved to be a powerful tool to explore the relationship among the structural, magnetic and superconducting transitions of iron-based superconductors [17–22], is necessary in understanding the peculiar superconductivity in these compounds. In the present work, we report a detailed ^{57}Fe Mössbauer study of La-doped $Ca_{1-x}La_xFe_2As_2$($x = 0.2$,0.3) compounds. The distributions of quadruple splitting provide strong support for phase separations in both compounds. With decreasing temperature, the La-rich phase suffers directly from superconducting transition while magnetic fluctuations and/or spin-phonon coupling may appear in the La-poor phase at temperatures slightly above T_c. These observations provide useful information for a better understanding of the observed superconductivity in these superconductors.

Experimental method

Single crystals of electron-doped $Ca_{1-x}La_xFe_2As_2$($x = 0.2$,0.3) superconductors were grown using FeAs self-flux method. The FeAs precursor was first prepared by reacting stoichiometric amounts of Fe and As powders sealed inside an evacuated quartztu be at 973 K for 20 h. Ca and La pieces were mixed with the FeAs powders according to the molar ratio of($Ca_{1-x}La_x$):FeAs = 1 : 4 and placed in an alumina crucible then sealed inside an evacuated quartz tube. All the weighing and mixing procedures were performed in a glove box filled with argon atmosphere. The assembly was slowly heated to 1473 K and held for 5 h, then cooled to 1173 K over 60 h before shutting down the furnace. Single crystals with flat shiny surface up to $5 \times 5\,mm^2$ can be obtained by cleaving the as-grown crystals for further measurements.

Transmission Mössbauer spectra (MS) at temperatures between 15 K and 300 K were recorded using a conventional constant acceleration spectrometer with a γ-ray source of25 mCi^{57}Co in palladium matrix. The absorber was composed of several small crystals with ~50 μm in thickness, which

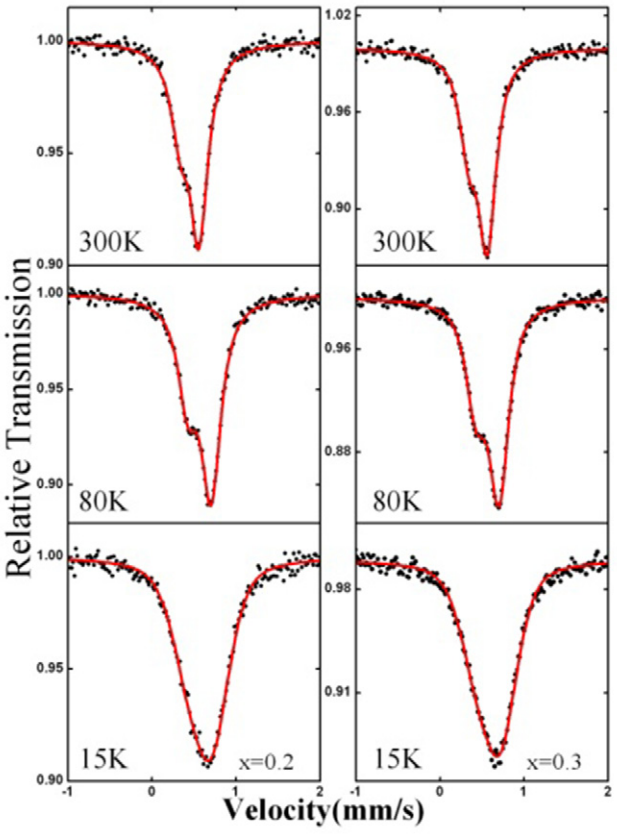

Figure 2. The^{57}Fe Mössbauer spectra of $Ca_{1-x}La_xFe_2As_2$ ($x = 0.2$, 0.3) and the fitted results using an asymmetric doublet at different temperatures.

is equivalent to ~10 mg cm^{-2} natural Fe. The absorber was arranged perpendicular to the γ-ray direction to take the crystal c-axis parallel to the γ-ray direction. During the measurements, the absorber was kept static in a temperature controllable cryostat filled with helium gas. The isomer shifts quoted in this work were converted relative to that of α-Fe.

Results and discussion

The qualities of the single-crystal samples of $Ca_{1-x}La_xFe_2As_2$ ($x = 0.0$, 0.2, 0.3) were checked by room temperature x-ray diffraction (XRD) using a Philips X′Pert diffractometer with Cu kα radiation (figure 1).Only sharp peaks along (0 0 l) orientation can be observed, indicating a high c-axis orientation of the single crystals. With La doping, the peaks shift slightly toward higher angle side, suggesting a successful chemical substitution of La for Ca ion which results in decrease of the c-axis lattice. Our observations agree with previous report [12], and can be ascribed to the large ionic radius of La compared with that of Ca. No impurity peaks are observable, indicating the high purity of the samples.

The superconducting property of $Ca_{1-x}La_xFe_2As_2$ compound was checked by standard electrical resistivity measurement using the standard four-probe technique under zero magnetic field. In samples with doping level $x = 0.2$ and $x = 0.3$, the resistivity data show a superconducting transition

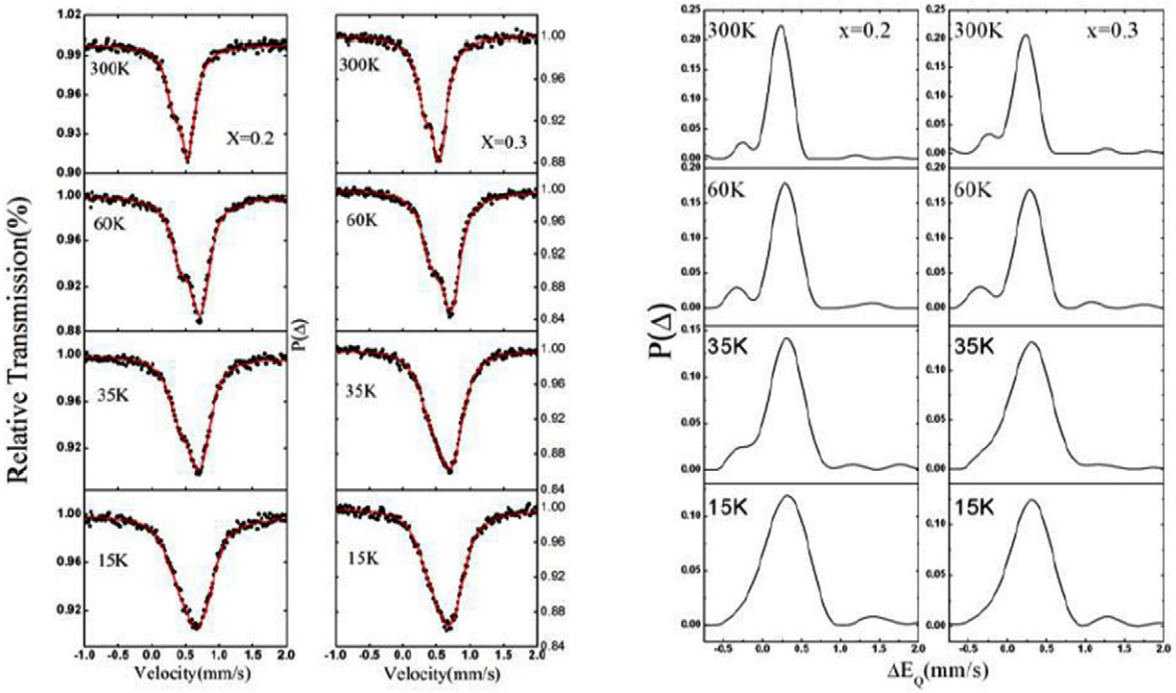

Figure 3. The ^{57}Fe Mössbauer spectra and the fitted results using the QSD method at different temperatures (a) and the distributions of quadrupole splitting ΔE_{Q} at indicated temperatures (b) for $Ca_{1-x}La_xFe_2As_2(x = 0.2, 0.3)$ compounds.

temperature T_{c} around 42K and 39 K, respectively (inset of figure 1). No anomaly due to the magneto-structural transition can be seen in the resistivity curves. The transition temperatures are similar to previously reported results [12, 13].The fact that the sample with larger doping level exhibits a little bit lower T_{c} suggests that the $x = 0.2$ and 0.3 samples correspond to under doped and over doped situations, respectively (see [12] for a doping dependent phase diagram).

The ^{57}Fe Mössbauer spectra of $Ca_{1-x}La_xFe_2As_2$ ($x = 0.2$, 0.3) single crystals at indicated temperatures are presented in figure 2 (black dots). For our single crystal mosaic samples, the crystal c-axis is parallel to the propagation orientation of γ-ray, which induces asymmetric quadrupole spectra. Actually, the Mössbauer spectra can be well fitted with an asymmetric doublet from room temperature to 15 K, indicating the absence of static magnetic order in the two compounds to the limit temperature of our measurements. It is found that the attempts of including common impurities such as FeAs, Fe_2As, and $FeAs_2$during the fitting procedure are not valid to improve the accuracy of the fitting, which also confirms the high purity of the samples.

It is well known that a Mössbauer spectrum is quite sensitive to the local chemical and crystallographic environments of the Mössbauer atoms. Considering the high concentration of the dopant atoms in the samples, the Fe atoms may experience a range of local environments provided that the La dopants distribute heterogeneously. Each distinct chemical and crystallographic environment contributes one pair of Lorentzian lines to the Mössbauer spectrum, which leads to a continuous distribution of quadrupole splitting. To get more information about the local environments of Fe atoms, it is reasonable to adopt the quadrupole splitting distribution (QSD) method to analyze the Mössbauer spectra of the $Ca_{1-x}La_xFe_2As_2$ compounds. The Voigt-based QSD method was applied here [23, 24]. This method uses a certain number of generalized sites and each normalized site-specific QSD is made up of a certain number of Gaussian components. In this method the isomer shift couples linearly with the quadrupole splitting, as $\delta = \delta_{0i} + \eta_i\Delta$, and the distribution of the quadrupole splitting can be expressed as $P(\Delta) = \Sigma p_i G_i(\Delta_{0i},\Gamma\Delta_i, \mathrm{A}_i;\Delta)$, where δ_0 is the isomer shift when Δ is zero, η is the coupling constant, p_i is the weight factor for the Gaussian (G_i) with area A_i and width $\Gamma\Delta_i$ centered at Δ_{0i}. The fitting line shape is a sum of Voigt lines. Since in a QSD analysis the line width Γ has a precise physical meaning, it is taken to be the same for all sites and was fixed as 0.234 mm s^{-1} here, a typical value for a Lorentzian line width for α-iron using the same radioactive source in our laboratory.

All the Mössbauer spectra of $Ca_{1-x}La_xFe_2As_2(x = 0.2, 0.3)$ compounds can be fitted well with the QSD method, as shown by the red solid lines in figure 3(a) at selected temperatures, where $\Delta E_{\mathrm{Q}} = \mathrm{e}QV_{ZZ}/2$. For both samples during the temperature region from room temperature to 60 K, the profiles of QSDs can be decomposed into two contributions (figure 3(b)) which are named according to the sign of ΔE_{Q} of the dome peak as positive component and negative component hereinafter. At room temperatures, the positive component is massive and centered around 0.31 mm s^{-1}, close to the reported ΔE_{Q} of the parent compound $CaFe_2As_2$ [25], the negative component is centered around -0.32 mm s^{-1} with the area ratio about 9.0% for both samples. The QSDs of the two $Ca_{1-x}La_xFe_2As_2$ samples exhibit similar evolutions with decreasing temperature. There is no abnormality observed until ~60 K, below which the positive dome broadens gradually with fixed peak

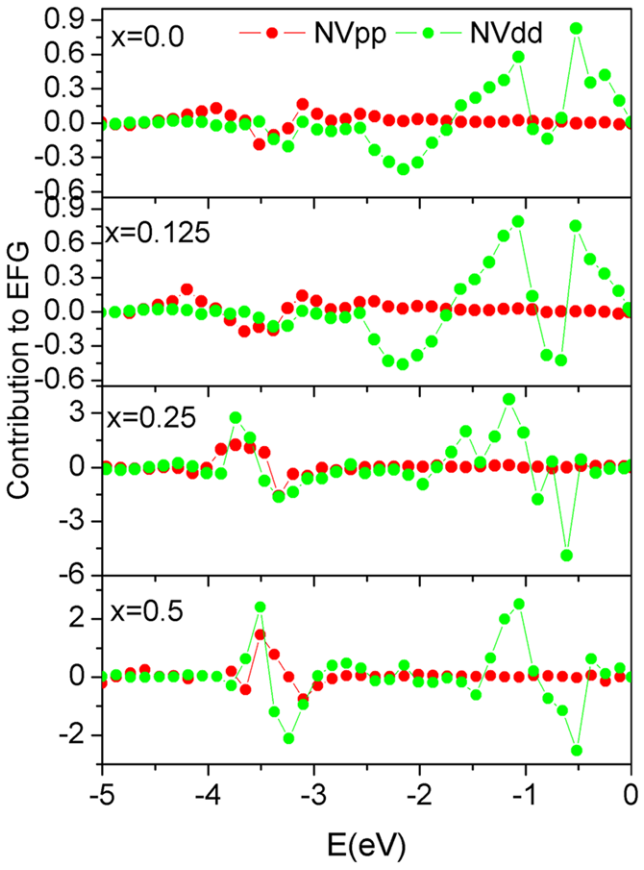

Figure 4. The evolutions of V_{ZZ}^{pp} and V_{ZZ}^{dd} with the state of energy for $Ca_{1-y}La_yFe_2As_2(y = 0, 0.125, 0.25, 0.5)$ compounds.

position. When it is very close to the critical temperature Tc, an abrupt rightward shift of the negative dome starts. Soon below Tc, it is hard to distinguish the negative dome from the positive one due to its small area ratio.

Considering the high purity of the samples and the temperature dependant behaviors of the QSDs, the negative component can't be ascribed to the impurities in the samples. To understand the origin of the negative component of QSD, we performed first principles calculations about the electronic structures and the electric field gradient (EFG) of $Ca_{1-y}La_yFe_2As_2(y = 0.125, 0.25, 0.5)$ model systems. The full potential linearized augmented plane wave (FP-LAPW) method as embodied in the WIEN2K code in a scalar relativistic version without spin–orbit coupling was adopted [26, 27]. Details of calculation methods can be found in [28]. At each doping level, several configurations can be founded. To mimic the situation of homogeneous distribution of the dopant atoms, the one with the highest symmetry was carefully chosen as the model system for further calculations. All model systems were optimized and the atomic coordinates were fully relaxed using the conjugate-gradient algorithm until the maximum force on a single atom is less than 1mRy $Å^{-1}$.

For $CaFe_2As_2$ compound, a tetragonal to collapsed tetragonal phase transition happens if Ca ion is substituted by rare earth element with smaller ion radius at proper doping level [12]. It is confirmed that the collapse happens when the interlayer As–As distance reaches the critical value of 3.0 Å, independently of the dopant. Since the ion radius of La^{3+} is larger than that of Ca^{2+}, no collapse phase transition should be expected in $Ca_{1-y}La_yFe_2As_2$ systems. According to our calculations, the tetragonal symmetry of the parent compound retains for all model systems and all have nonmagnetic ground state. It is found that the lattice constants a increase slightly with increasing doping content, which is consistent with experiments [12]. For $Ca_{0.75}La_{0.25}Fe_2As_2$, for example, the calculated lattice parameters $a = 4.00$ Å, $c = 11.05$ Å, $d_{As-As} = 3.14$ Å, match well with the experiments. The main results of the calculations yield V_{zz} ($\times 10^{21}$ V m^{-2}), the principle component of EFG, of 0.297, −0.319 and −0.573 for $y = 0.125$, 0.25, 0.5, respectively. Obviously, V_{zz} changes from positive to negative with increasing La content.

To capture the details of EFG in $Ca_{1-y}La_yFe_2As_2$ system, we decomposed the EFG at iron site into the contributions of p–p interaction and d–d interaction, named as V_{ZZ}^{pp} and V_{ZZ}^{dd}, respectively. Figure 4 shows the calculated evolutions of the two terms with the state of energy for $Ca_{1-y}La_yFe_2As_2$ systems, where the EFG of the parent compound is also shown for the convenience of comparison. Obviously, the contribution from d–d interaction is dominant for all systems, especially from the d-t_{2g} orbitals near the Fermi energy. The profiles of V_{ZZ}^{pp} and V_{ZZ}^{dd} of $y = 0.125$ system are quite similar to those of the parent and the sum of the energy integrals of the two terms yields positive V_{zz}. But the energy dependence of V_{ZZ}^{pp} and V_{ZZ}^{dd} are quite different for $y = 0.25$ and $y = 0.5$ systems, especially in the energy region close to the Fermi level, and the sum of the energy integrals yields negative V_{zz}.

The switch of the V_{zz} sign can be well explained in terms of charge redistribution of Fe-3d electrons with doping level. Generally, EFG is determined by the non-spherical charge-density as well as the radial dependence of the anisotropic charge density. In $CaFe_2As_2$ parent compound, an iron atom is in the center of a slightly distorted tetrahedron cage formed by four As atoms. To describe the distortion of the FeAs tetrahedron, we calculated the angle θ formed by the iron atom cornered by two As atoms with the same c-coordinate in the tetrahedron. It is found that θ increases from 109.8° for $y = 0.0$ to 119.4° for $y = 0.5$, which means the FeAs tetrahedron is flattened along the c-axis by La doping. This kind of distortion will directly influence the band structures of Fe-3d electrons near the Fermi level. We calculated the occupation number of each Fe-3d orbital and find that, with increasing La content, the electrons move from the d_{xy} orbital to the d_{yz} and d_{xz} orbitals, namely, from the ab-plane to out-of-plane. The charge redistribution changes the spatial symmetry of 3d electrons and switches the sign of V_{zz} at proper La content. This orbital-dependent electronic structure reconstruction has been observed by polarization-dependent angle-resolved photoemission spectroscopy measurements and band calculations [29, 30].

Under the direction of the theoretical calculations, the experimental QSDs of $Ca_{1-x}La_xFe_2As_2$ compounds can be well understood. For a homogeneous doping system, one QSD would be produced. For systems with high doping concentration, like the two $Ca_{1-x}La_xFe_2As_2$ compounds in the

present work, heterogeneous distributions of La atoms may occur which naturally produce variations in the local environments of iron atoms. Therefore, multiple QSDs are formed in the Mössbauer spectra. According to the calculations, it is reasonable to ascribe the positive QSD component to the contributions from Fe atoms with comparatively less La neighbors, while the negative QSD component comes from Fe atoms with comparatively more La neighbors.

The Fermi surface reorganization caused by the formation of superconducting gap leads to redistributions of Fe-3*d* electrons in iron pnictids, which may induce observable modifications in V_{zz} around the transition temperature [31]. As mentioned above, the negative QSD dome moves rightward abruptly at T_c and soon merges into the positive dome below T_c. Therefore, it is reasonable to ascribe the abnormal behavior of the negative QSD component around T_c to the superconducting transition happened in regions rich in La dopants. On the other hand, the positive QSD component changes smoothly around T_c, implying that the regions with poor La dopants do not take part in superconducting. Note that the area ratio of the negative QSD dome is about 9%, which is similar to recent reports about a very small superconducting volume in La-doped $Ca_{1-x}La_xFe_2As_2$ [32, 33] and $Ca_{1-x}Pr_xFe_2As_2$ [16] superconductors. Suppose the average doping content is 0.25 for the La-rich phase, the average doping concentration can be estimated to be ~0.05 for the La-poor phase, which is far away from the superconducting region in the doping phase diagram. Thus the superconductivity in $Ca_{1-x}La_xFe_2As_2$ should be inhomogeneous in nature. Our observations provide new evidence in explaining the very small superconducting volume fraction of these superconductors.

Whether magnetic and superconducting regions reside in nanoscopically separated phases or coexist on an atomic scale has attracted intense study since the discovery of high temperature superconductivity in iron pnictides. Hence it is interesting to explore the possibility of magnetic fluctuation in La-poor regions. For this purpose, we turn to the hyperfine parameters obtained from an asymmetric doublet fitting of the measured Mössbauer spectra of the two samples.

Since the crystal field splitting influences the spin state of Fe^{2+} in iron pnictides, we focus on the temperature dependence of the quadruple splitting ($eQV_{zz}/2$) (figure 5(a)) to deduce the tetragonal splitting of Fe-t_{2g} orbitals. All parent compounds of iron pnictides have the electronic configuration Fe d^6 and the tetrahedral crystal field splits the free-ion Fe^{2+} ground term into a low-lying doublet e_g and a higher triplet t_{2g} (d_{xy}, d_{xz}, d_{yz}) separated by ~0.2 eV [26].The irregularity of the FeAs tetrahedron induces a further splitting of t_{2g} levels, that is, d_{xz} + d_{yz} orbitals are pushed to higher energy side and the d_{xy} orbital is slightly lowered. As mentioned above, the main contributions to the V_{zz} of iron site come from the t_{2g} orbitals near the Fermi energy, while the mixing of e_g state and t_{2g} state is expected to be small since the tetrahedral crystal field splitting is large (~0.2 eV) [29]. In this case, the V_{zz} can be expressed as the thermal average of contributions from the three t_{2g} orbitals [34], as

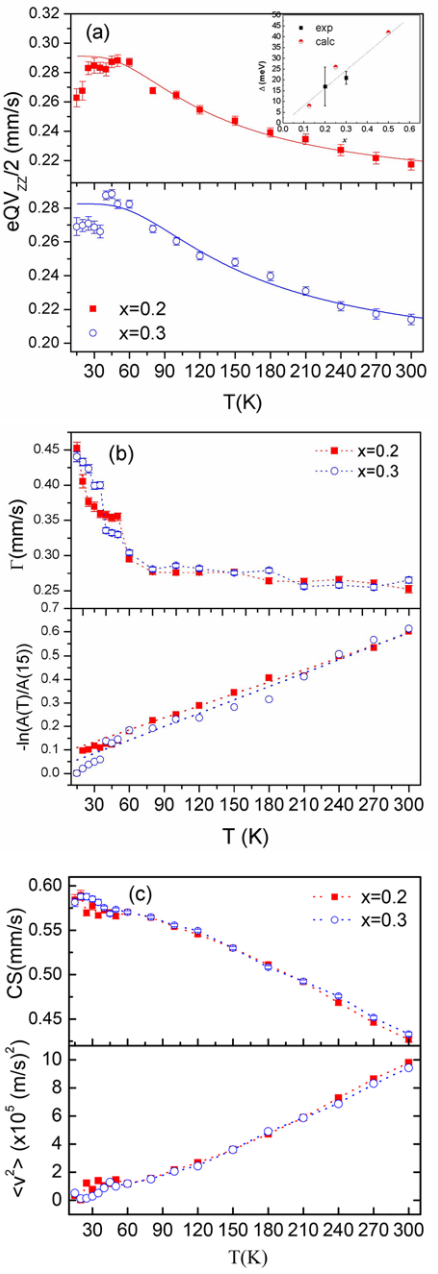

Figure 5. Temperature dependences of (a) $eQV_{zz}/2$ and the theoretical fittings (solid lines) using equation (2) described in the text; (b) the spectral line width Γ_{exp} and the spectral area, normalized to that at 15 K; (c) the center shift (CS) of the MS spectra and the deduced mean-square velocity for $Ca_{1-x}La_xFe_2As_2$ compounds. The dotted lines in (b) and (c) are intended as guides to the eyes only. The inset in (a) shows the energy splitting Δ of t_{2g} orbitals versus doping content.

$$V_{zz} = \frac{\sum_i (V_{zz})^i \exp\left[-\Delta_i/(k_B T)\right]}{\sum_i \exp\left[-\Delta_i/(k_B T)\right]} \quad (1)$$

where Δ_i is the energy of the ith orbital with respect to the ground state, $(V_{zz})^i$ is the contribution from orbital di. For simplicity, we adopt the expectation values of $(V_{zz})^l$ as pure Fe-3*d* orbitals [35] because the spin–orbit coupling produces a

small effect on the quadrupole splitting (~0.001 × 10^{21} V m^{-2} according to our DFT calculations). Setting d_{xy} as the ground state, one obtains

$$V_{zz}(T) = (V_{zz})_C + (V_{zz})(0)\frac{1-\exp[-\Delta/(k_BT)]}{1+2\exp[-\Delta/k_BT]} \quad (2)$$

where $(V_{zz})_C$ contains all temperature independent contributions, $V_{zz}(0)$ corresponds to the value at 0 K.

Analyzing the temperature dependence of $eQV_{zz}/2$ from room temperature to 60 K using equation (2) yields $\Delta = 17(9)$ meV for $x = 0.2$ and $\Delta = 21(3)$ meV for $x = 0.3$(see solid lines in figure 5(a)). Based on the calculated electronic band structures of $Ca_{1-y}La_yFe_2As_2$ model systems, we calculated the weighted center positions of d_{xy} and $d_{xz} + d_{yz}$ orbitals and evaluated the tetragonal splitting Δ_y as the difference between the two center positions, which yields $\Delta_{0.125} = 8$ meV, $\Delta_{0.25} = 26$ meV and$\Delta_{0.5} = 42$ meV. The results conforms to the theoretical calculations, see the inset of figure 5(a). We can see the splitting is rather small (Δ/J ~ 0.1 with J being the Hund's coupling constant [14]) in $Ca_{1-x}La_xFe_2As_2$ compounds, which favors nonzero spin states (S ≠ 0). Actually, Gretarsson found that the Felocal moment is about 0.9 μ_B at room temperature and remains unchanged with decreasing temperature in $Ca_{0.78}La_{0.22}Fe_2As_2$ using Fe K_β x-ray emission spectroscopy [14]. At low temperatures the correlations among the iron moments may result in short range magnetic fluctuations. Considering that the positive QSD component contains 91% of iron atoms in the samples, the hyperfine parameters deduced via one doublet fitting represent the information of the La-poor phase.

On the basis of the temperature dependences of the line width, the spectra area and the center shift (CS), it seems that magnetic fluctuations and/or spin-phonon coupling appear in La-poor regions at temperatures slightly above T_c in $Ca_{1-x}La_xFe_2As_2$ superconductors. Figure 5(b) displays the temperature dependences of the spectral line width Γ_{exp}(T) (upper panel), together with the relative spectral area ln(A(T)/A(15)) (bottom panel), where A(15) being the spectral area measured at 15 K. As can be seen, for each compound, Γ_{exp}(T) is almost constant with decreasing temperature till ~60 K below which a sudden upturn happens. Simultaneously, ln(A(T)/A(15)) manifests an anomaly in the increasing tendency.

There are several reasons which can result in line width broadening of the Mössbauer spectra, such as: (1) disorder and/or inhomogeneous substitution induced distributions of hyperfine parameters (including mainly the isomer shift, the quadruple splitting and the hyperfine magnetic field); (2) the onset of short-range magnetic fluctuations; (3) the appearance of spin-phonon coupling. As mentioned above, though the peak position of the positive QSD component is hardly moved, the profile gets flattened below 60 K, indicating the distributions of quadruple splitting in this phase. But the quadruple splitting distribution alone does not cause extra increase in the spectral area. Usually the sudden increase in the spectra area is an indicator of the appearance of magnetism due to saturation effect, i.e. the magnetic splitting of the energy levels of a ^{57}Fe nucleus always accompanies an abrupt expansion of the spectral area [36]. However, magnetically splitting is not observable till the limit temperature of the present measurements.

We suggest that the line width broadening observed here is likely due to the appearance of short-range spin nematic fluctuations in these compounds. Strong low-energy spin nematic fluctuations have been observed at temperatures much higher than structural/magnetic phase transition temperatures in iron pnictides [37, 38]. Synchrotron Mössbauer spectroscopy detected short-range magnetic transition in the tetragonal phase in $BaFe_2As_2$ [20]. It is found that for hole-doped and electron-doped 122-type iron pnictides, superconductivity is even adjacent to nematic fluctuations near optimum doping region [39, 40]. These facts strongly suggest the significance of nematic order in the evolution from magnetic phase to superconducting state.

Within the general framework of spin nematic fluctuations, the emergence of EFG distributions around 60 K is expected. There are three types of nematic instabilities according to the origin: structural, orbital and spin-driven nematic order. No matter which one drives the nematic instability, the three order parameters must be present simultaneously because the order parameters are bi-linear combinations [41]. There is general agreement among researchers that magnetic fluctuations drive the nematic instability in iron pnicdtides, which spontaneously break the tetragonal symmetry of the system and induce nematicity in orbital order [42].The orbital nematicity could arise charge redistribution between localized d_{xy} orbitals and itinerant d_{xz}/d_{yz} orbitals, which results in EFG distributions since, as mentioned above, these three orbitals contribute most to the EFG of these compounds.

Besides orbital nematic fluctuations, structural distortion, which is normally associated with a phonon-driven structural transition, is also expected and the spin-phonon coupling can be detected by Mössbauer spectroscopy due to its high energy resolutions. Close investigations of the recoil-free factor f and the CS of the MS spectra provide traces of spin-phonon coupling in both $Ca_{1-x}La_xFe_2As_2$ samples. In the thin-absorber approximation, the recoil-free factor f is related to the mean-square amplitude of vibrations $\langle x^2\rangle$ of the Mössbauer atoms as $f = \exp(-\langle x^2\rangle k^2)$, while the CS of the spectra is related to the mean-square velocity $\langle v^2\rangle$ of the vibrating atoms via the second-order Doppler shift (SOD) as $SOD = -E_\gamma\langle v^2\rangle/2c^2$, where E_γ is the energy of the gamma rays. As shown in figures 5(b) and (c), both $-ln(A(T)/A(15))$ and CS deviate from the dotted lines expanded from the high temperature behaviors below 60 K. Obviously, the decreasing tendencies of $\langle x^2\rangle$ and $\langle v^2\rangle$ stagnate, suggesting the appearance of spin-phonon interaction. Recently, spin-phonon coupling has been observed by Raman scattering study on a similar compound $Ca_{0.88}Pr_{0.12}Fe_2As_2$ [43].

The fact that no magnetic fluctuations have been detected in $Ca_{1-x}La_xFe_2As_2$ by neutron scattering may be due to two factors: first, the nematic fluctuations are hindered by the heterogeneously distributed La-rich regions in the compounds and the fluctuations may behave like magnetic clusters relaxation;

and second, the average size of the nematic clusters is far smaller than the neutron-scattering value (~10 nm) but can be observed by the Mössabuer spectrum [44].

Conclusions

In summary, we have studied the La-doped $Ca_{1-x}La_xFe_2As_2$ ($x = 0.2$, 0.3) superconductors using ^{57}Fe Mössbauer spectroscopy and first principles calculations. According to the theoretical calculations of the electronic structures and V_{zz} of the $Ca_{1-y}La_yFe_2As_2$($y = 0.125$, 0.25,0.5) model systems, the V_{zz} experienced by iron nucleus changes from positive to negative, which is ascribed to the charge repopulation among t_{2g}orbitals induced by the increasing tetragonal splitting with doping level. The QSDs of $Ca_{1-x}La_xFe_2As_2$ compounds provide evidence of heterogeneous distribution of the La atoms. According to the temperature dependence of QSDs, it is clear that the La-rich phase and the La-poor phase is separated spatially and it is the La-rich phase that undergoes superconducting transition with decreasing temperature. If this is indeed the case, it will be interesting to determine the similarities and differences in pairing mechanism between the Re-doped $CaFe_2As_2$ superconductors and other 122-type pnictides. More experiments based on local probes are desired to check this picture.

Acknowledgments

This work is supported by the National Natural Science Foundation of China under Grant No. 11275086.

References

[1] Berry N, Capan C, Seyfarth G, Bianchi J Q, Ziller J and Fisk Z 2009 *Phys. Rev.* B **79** 180502
[2] Nandi S *et al* 2010 *Phys. Rev. Lett.* **104** 057006
[3] Putzke C *et al* 2014 *Nat. Commun.* **5** 5679
[4] Kim M G *et al* 2011 *Phys. Rev.* B **83** 054514
[5] Li Z W, Ma X M, Pang Hand Li F 2012 *Chin. Phys.* B **21** 047601
[6] Mazin I I, Singh D J, Johannes M D and Du M H 2008 *Phys. Rev. Lett.* **101** 057003
[7] Evtushinsky D V *et al* 2009 *Phys. Rev.* B **79** 054517
[8] Ding H *et al* 2008 *Europhys. Lett.* **83** 47001
[9] Takahashi H, Soeda H, Nukii M, Kawashima C, Nakanishi T, Limura S, Muraba Y, Matsuishi S and Hosono H 2015 *Sci. Rep.* **5** 7829
[10] Sun L *et al* 2012 *Nature* **483** 67
[11] Kudo K, Iba K, Takasuga M, Kitahama Y, Matsumura J I, Danura M, Nogami Y and Nohara M 2013 *Nature* **3** 1478
[12] Saha S R, Butch N P, Drye T, Magill J, Ziemak S, Kirshenbaum K, Zavalij P Y, Lynn J W and Paglione J 2012 *Phy. Rev.* B **85** 024525
[13] Zhao S G, Yan P Q, Lei W, Dong L W, Xian P Z, Chao Y, Chun L W and Yan W M 2011 *Europhys. Lett.* **95** 67002
[14] Gretarsson H, Saha S R, Drye T, Paglione J, Kim J, Casa D, Gog T, Wu W, Julian S R and Kim Y-J 2013 *Phys. Rev. Lett.* **110** 047003
[15] Zeljkovic I, Dennis H, Song C L, Lv B, Chu C W and Hoffman J E 2013 *Phys. Rev.* B **87** 201108
[16] Gofryk K, PanM H, Cantoni C, Saparov B, Mitchell J E and Sefat A S 2014 *Phys. Rev. Lett.* **112** 047005
[17] Long G, DeMarco M, Chudyk M, Steiner J, Coffey D, Zeng H, Li Y K, Gao G H and Xu Z A 2011 *Phys. Rev.* B **84** 064423
[18] Nowik I and Felner I 2009 *Physica* C **469–85** 490
[19] Blachowski A, Ruebenbauer K, Zukrowski J, Rogacki K, Bukowski Z and Karpinski J 2011 *Phys.Rev.* B **83** 134410
[20] Wu J J, Lin J F, Wang X C, Liu Q Q, Zhu J L, Xiao Y M, Chow P and Jin C Q 2013 *Proc. Nat. Acad. Sci. USA* **110** 17263–6
[21] Wu J J, Lin J F, Wang X C, Liu Q Q, Zhu J L, Xiao Y M, Chow P and Jin C Q 2014 *Sci. Rep.* **4** 3685
[22] Bi W L *et al* 2015 *Synchrotron Radiat.* **22** 760–5
[23] Ping J Y, Rancourt D G and Stadnik Z M 1991 *Hyperfine Interact.* **69** 493
[24] Rancourt D G 1994 *Phys. Chem. Miner.* **21** 244–249
[25] Alzamora M, Munevar J, Baggio-Saitovitch E, Bud'ko S L, Ni N, Canfield P C and Sánchez D C 2011 *J. Phys.: Condens. Matter* **23** 145701
[26] Blaha P, Schwarz K, Sorantin P and Trickey S B 1990 *Comput. Phys. Commun.* **59** 399
[27] Blaha P, Schwarz K, Madsen G, Kvasnicka D and Luitz J 2001 *WIEN2K* www.wien2k.at
[28] Li Z W, Fang Y, Ma X M, Pang H and Li F S 2011 *Phys. Rev.* B **84** 134509
[29] Andersen O K and Boeri L 2011 *Ann. Phys., Lpz.* **523** 8–50
[30] Zhang Y *et al* 2012 *Phys. Rev.* B 85085121
[31] Jasek A K, Komedera K, Błachowski A, Ruebenbauer K, Bukowski Z, Storey J G and Karpinski J 2014 *J. Alloy. Compd.* **609** 150–5
[32] Saha S *et al* 2014 *Phys. Rev.* B **89** 134516
[33] Tamegai T, Ding Q P, Ishibashi T and Nakajima Y 2013 *Physica* C **484** 31–4
[34] Hutchings M T 1964 *Solid State Phys.* **16** 227
[35] Perkins H K and Hazonyt Y 1972 *Phys. Rev.* B **5** 7–18
[36] Kolk B, Bleloch A and Hall D 1986 *Hyperfine Interact.* **29** 1377
[37] Fu M, Torchetti D A, Imai T, Ning F L, Yan J-Q and Sefat A S 2012 *Phys. Rev. Lett.* **109** 247001
[38] Kasahara S *et al* 2012 *Nature* **486** 382–5
[39] Fernandes R M, VanBebber L H, Bhattacharya S, Chandra P, Keppens V, Mandrus D, McGuire M A, Sales B C, Sefat A S and Schmalian J 2010 *Phys. Rev. Lett.* **105** 157003
[40] Fernandes R M, Chubukov A V, Knolle J, Eremin I and Schmalian J 2012 *Phys. Rev.* B **85** 024534
[41] Fernandes R M, Chubukov A V and Schmalian J 2014 *Nat. Phys.* **10** 97–104
[42] Fernandes R M and Schmalian J 2012 *Supercond. Sci. Technol.* **25** 084005
[43] Hartmann-Boutron F, Aït-Bahammou A and Meyer C 1987 *J. Physique* **48** 435–44
[44] Litvinchuk A P, Lv B and Chu C W 2011 *Phys. Rev.* B **84** 092504